

Synthesis and Photophysical Properties of a Conformationally Flexible Mixed Porphyrin Star-Pentamer

Toby D. M. Bell,^A Sheshanath V. Bhosale,^B Kenneth P. Chiggino,^A Steven J. Langford,^{B,C} and Clint P. Woodward^B

^ASchool of Chemistry and Bio21 Institute, The University of Melbourne, Parkville, Vic. 3010, Australia.

^BSchool of Chemistry, Monash University, Clayton, Vic. 3800, Australia.

^CCorresponding author. Email: s.langford@sci.monash.edu.au

The synthesis of a porphyrin star-pentamer bearing a free-base porphyrin core and four zinc(II) metalloporphyrins, which are tethered by a conformationally flexible linker about the central porphyrin's antipody, is described. The synthetic strategy is highlighted by the use of olefin cross metathesis to link the five chromophores together in a directed fashion in high yield. Photoexcitation into the Soret absorption band of the zinc porphyrin chromophores at 425 nm leads to a substantial enhancement of central free-base porphyrin fluorescence, indicating energy transfer from the photoexcited zinc porphyrin (outer periphery) to central free-base porphyrin. Time-resolved fluorescence decay profiles required three exponential decay components for satisfactory fitting. These are attributed to emission from the central free-base porphyrin and to two different rates of energy transfer from the zinc porphyrins to the free-base porphyrin. The faster of these decay components equates to an energy-transfer rate constant of $3.7 \times 10^9 \text{ s}^{-1}$ and an efficiency of 83%, whereas the other is essentially unquenched with respect to reported values for zinc porphyrin fluorescence decay times. The relative contribution of these two components to the initial fluorescence decay is $\sim 3:2$, similar to the 5:4 ratio of *cis* and *trans* geometric isomers present in the pentamer.

Manuscript received: 11 March 2009.

Final version: 13 May 2009.

Introduction

The efficient synthesis of multiporphyrin systems, ranging from dimers to higher oligomers, is sought for applications in light-harvesting,^[1] two-photon absorption spectroscopy,^[2] catalysis^[3] and molecular recognition applications,^[4] and for studying hole and energy transfer reactions.^[5] Linking of porphyrin chromophores by covalent bonds to form stable, multiporphyrin architectures has previously been achieved using several different porphyrin-to-porphyrin coupling techniques,^[6] yet alternative methods suitable for forming regiospecifically mixed-metal (or metal-free-base) porphyrin architectures and systems containing sensitive pendant functional groups are still sought. Our interest in this area also stems from the fact that multichromophoric systems that undertake a single donor and acceptor event from an array of potential donors allow what is termed a *redundancy effect* to be evaluated.^[1f] If, or when, one of the donors is damaged, another is there to take its place, maintaining the cycle and facilitating longevity in the device application.

Recently, we have been studying the use of olefin cross metathesis (CM) as a mild coupling technique to prepare donor-acceptor systems^[7] by taking advantage of the differences in olefin reactivity.^[8] Olefin CM has also been found to be an effective tool for the covalent capture of supramolecular porphyrinic architectures.^[9] Here, we report the extension of this CM coupling strategy to the synthesis of a star-burst,

mixed pentameric porphyrin array (**1**) and discuss a preliminary photophysical analysis of this light-harvesting complex mimic.

Results and Discussion

Synthesis of the Star-Burst Pentamer **1**

Our previous work in the formation of a porphyrin-C₆₀ dyad and multiporphyrin arrays using CM demonstrated that 3-butenyl phenyl and α,β -unsaturated ester olefins are ideal coupling partners. Once the mixed cross-product is formed, it can no longer be reactivated by the catalyst,^[8] thereby trapping out the desired chromophore bridge with excellent chemo- and stereoselectivity. The 3-butenyl phenyl groups were also specifically chosen to minimize olefin isomerization under metathesis conditions.^[10] Porphyrin **2**, bearing four *meso* 4-(3-butenyl)phenyl groups, was prepared from the reaction of pyrrole with the aldehyde **3**^[9b] under Rothmund conditions in 20% yield. The corresponding zinc metallated adduct **4** was subsequently formed using standard metallation conditions.^[11] The mono acryloyl functionalized porphyrin cross partner **5** was prepared according to a previously reported method in an 8% yield over two steps (Scheme 1).^[7a] Zinc(II) metallation of **5** was achieved using Zn(OAc)₂ in CH₃CN/CHCl₃ to give **6** in a 70% yield after purification by column chromatography. The substitution of methanol for acetonitrile as the co-solvent of choice in this case was

necessary to avoid any transesterification of the acryloyl ester functionality.

In a model reaction, zinc(II) porphyrin **4** was reacted with an excess of methyl acrylate in the presence of second-generation Grubbs' catalyst (20 mol-%, 5 mol-% per alkene). After 2 days, the corresponding tetrafunctionalized product **7** was isolated in 63% yield by column chromatography (SiO₂, 20:1 CHCl₃/acetone) (Scheme 2). In line with our previous work, only the *trans* isomer was observed by ¹H NMR spectroscopic analysis for the newly installed acrylate functionality.

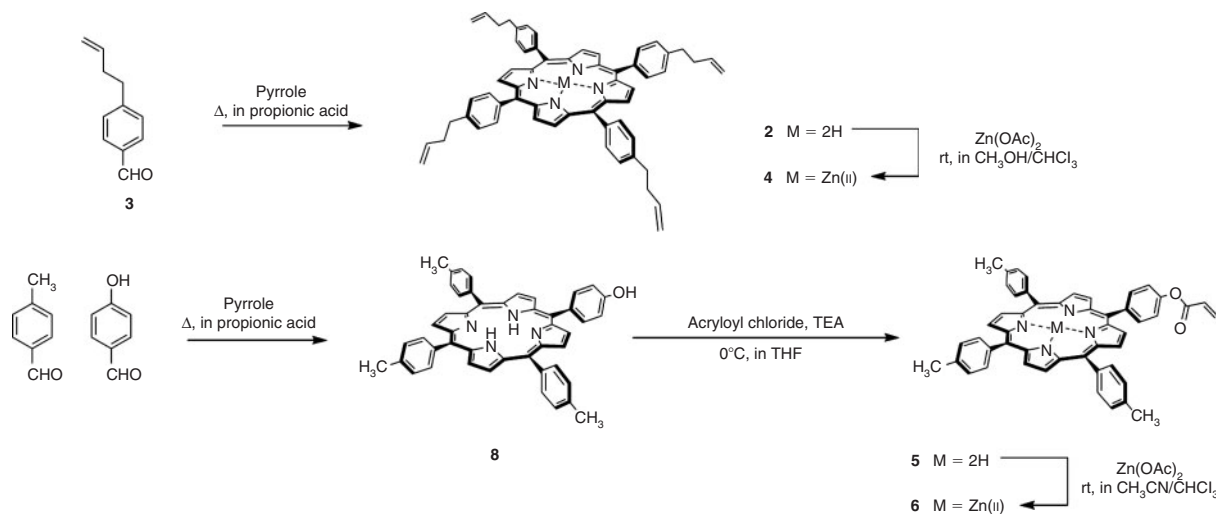
With suitable conditions in hand, the zinc(II) (4-acryloyloxy)phenylporphyrin (**6**) and the free-base butenyl functionalized porphyrin (**2**) were combined in a 6:1 ratio under metathesis conditions to effect formation of the mixed-porphyrin pentamer (Scheme 3). A high loading of the second-generation Grubbs' catalyst (50 mol-% catalyst present per alkene linkage) was employed to ensure a short reaction time. Formation of the pentamer **1** proceeded smoothly, with the complete disappearance of the porphyrin **2** within the first 2 h of the reaction, as determined by TLC analysis. After 24 h, two major bands were detected by TLC analysis, one corresponding to the excess porphyrin acrylate **6** and a second broad porphyrinic band of significantly lower R_F value. The second band was isolated by column chromatography (CHCl₃/acetone, 50:1) to yield the desired mixed star pentamer **1** in 84% yield.

Assessment of the ¹H NMR spectrum of **1** revealed reasonably few unique resonance signals, which indicated the

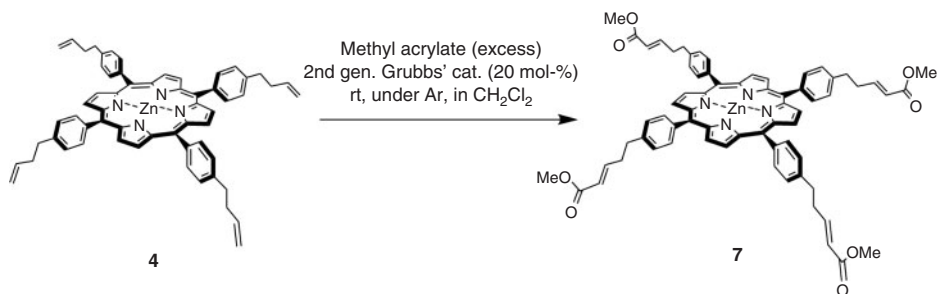
formation of a highly symmetrical product (Fig. 1). Loss of the olefinic proton resonances of porphyrins **2** and **6** and the appearance of two new resonance signals at 6.08 and 6.24 ppm indicated successful tetracoupling to the central porphyrin **2** had taken place. Furthermore, the proton resonance signals of the β-pyrrolic, inner-periphery NH, *meso* aromatic, and alkyl moieties were all accounted for in the ¹H NMR spectrum, displaying the expected integration values for the desired mixed pentamer product **1**. The olefinic resonance signals observed in the ¹H NMR spectrum of **1**, at 6.08 and 6.24 ppm were assigned as a mixture of *cis* and *trans* geometric isomers in approximately a 5:4 ratio. This was an unexpected result considering that all other hetero CM-mediated porphyrin modifications previously performed by our group have given exclusive *trans*-isomer formation. The poor *cis* and *trans*-isomer selectivity is attributed to a gradual increase in the steric bulk around the central free-base porphyrin **2** as the reaction progresses, forcing the catalyst to operate via a less-favoured stereochemical pathway. Laser desorption mass spectrometry provided further supporting evidence of the successful formation of the mixed porphyrin pentamer **1**, with the observed isotopic pattern closely matching that predicted for the structure (see Accessory Publication).

Steady-State Spectra

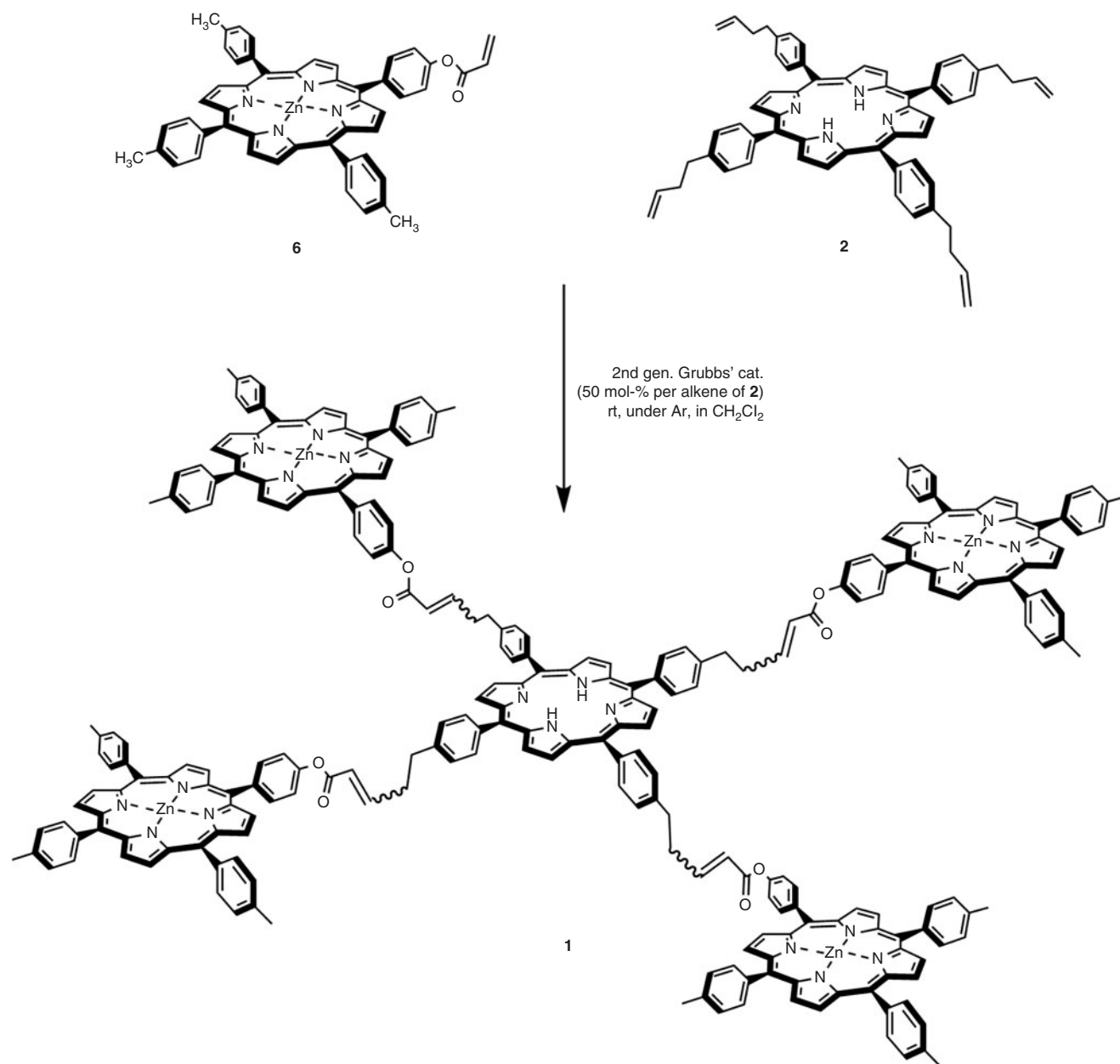
The absorption spectrum of **1** in toluene is shown in Fig. 2 and features a strong absorption band in the blue region of



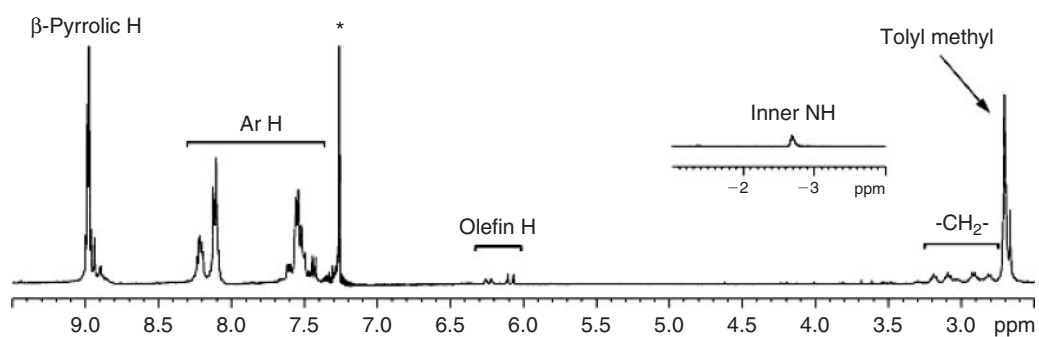
Scheme 1.



Scheme 2.



Scheme 3.

Fig. 1. 400 MHz ¹H NMR spectrum (273 K, CDCl₃) of the mixed porphyrin pentamer (**1**) isolated from the cross metathesis reaction.

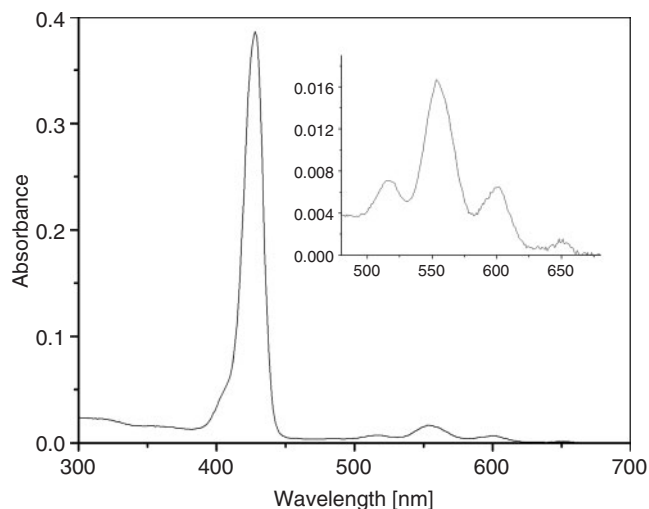


Fig. 2. Absorption spectrum of **1** in toluene. Inset shows the Q-band region in more detail.

spectrum (the Soret band – absorption to the second singlet state S₂), and a series of weaker absorptions at longer wavelengths (the Q-bands – absorption to the first excited singlet state S₁). Expansion of the Q-band region is shown in the inset of Fig. 2 and absorption maxima are apparent at 515, 553, 601, and 648 nm. Comparison of the spectra with those of typical zinc(II) (ZnP) and free-base (FbP) porphyrins (such as the much-studied tetraphenyl derivatives)^[12] suggests that for **1**, up to six absorption maxima in the Q-band region might be expected, two associated with the ZnP chromophores, and four due to the free-base chromophore (the different number of Q-bands for the two different types of porphyrin arises owing to the higher-order symmetry resulting from replacement of two protons by a central Zn^{II} cation). The observation of four Q-band absorption maxima suggests that there is significant spectral overlap of the ZnP and FbP bands, so that all maxima are not fully resolved. This overlap is also the likely cause of the slightly distorted shape of the bands in the observed absorption spectrum of **1**.

The emission spectrum of **1** in toluene is provided in Fig. 3a. With excitation at 425 nm, where ZnP and FbP absorb strongly, the spectrum shows features characteristic of both these chromophores. The emission maxima of Zn tetraphenylporphyrin (TPP) in toluene occur at 598 and 647 nm, and for FbTPP, which emits further to the red, maxima in toluene are at 649 and 717 nm.^[12a] Three emission bands are present (at 608, 654, and 721 nm) in the emission spectrum of **1** and can be assigned as follows: the band with a maximum at 608 nm is a higher-energy ZnP emission band, the peak at 721 nm is the lower-energy FbP emission band and the central band is a combination of the lower-energy ZnP band and the higher-energy FbP band. The relative intensity of the zinc porphyrin emission, however, is attenuated (i.e. quenched) considerably when compared with the free-base porphyrin (cf. comparison of intensity at 608 and 721 nm), particularly considering that there are four ZnP chromophores compared with a single FbP species. The quantum yield of fluorescence with excitation at 425 nm was determined to be 0.034.

Excitation spectra of **1** are presented in Fig. 3b. The fluorescence excitation spectrum obtained monitoring at 615 nm (Fig. 3b dashed line), where only the ZnP chromophores emit, and the spectrum obtained by monitoring at 730 nm, where emission is dominated by FbP, are quite similar. If the ZnP and FbP

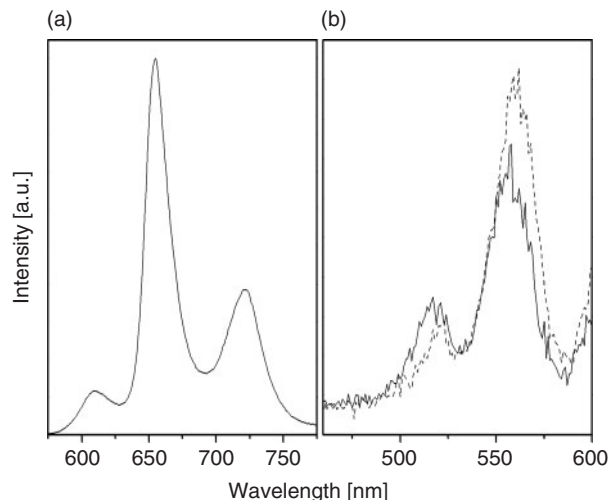


Fig. 3. (a) Corrected emission spectrum of **1** in toluene following excitation at 425 nm. The shortest and longest wavelength maxima can be assigned to emission from ZnP and FbP chromophores respectively, while the central band consists of overlapped emission bands from both chromophores. (b) Corrected excitation spectra (wavelengths <600 nm) of **1** in toluene monitoring fluorescence at 615 nm (dashed line) and 730 nm (solid line).

chromophores were emitting independently, then the excitation spectra would reflect the different absorption spectra of the two species. The quenched ZnP emission and the large contribution to the excitation spectrum of FbP imply that absorption by the peripheral ZnP chromophores is leading to emission from the central FbP chromophore, confirming that significant excitation energy transfer (EET) from the ZnP chromophores to the central FbP is occurring.

Time-Resolved Fluorescence Measurements

To investigate further the possibility of EET being operative in **1**, time-resolved fluorescence decay profiles were recorded using the time-correlated single-photon counting method at 15-nm wavelength intervals from 595 to 700 nm and at 720 nm. The decay profiles displayed a significant wavelength dependence that is most pronounced for the extreme cases of 595 and 720 nm, where emission is dominated by ZnP and FbP, respectively. These two emission decay profiles are shown in Fig. 4.

Based on the typical spectral characteristics of fluorescence emission from ZnP and FbP chromophores, contributions from both porphyrin species are expected over the wavelength range studied. In addition, the two decay profiles shown in Fig. 4 are clearly decaying over different time-scales. Based on literature fluorescence lifetimes,^[7b,13] decay components with decay time constants in the ranges of 10–12 ns (for FbP) and 1.4–1.7 ns (for ZnP) might reasonably be expected. Fitting the decay profiles with one or two exponential decay components did not yield satisfactory fits at all wavelengths – three components were required. The extracted decay constants showed very little variation across the nine decay profiles, which could, indeed, be fitted globally with quite satisfactory results in terms of both the local and global χ^2 fitting parameters (global $\chi^2 = 1.21$) and the randomness of the residuals for each profile. The residuals for the two decay profiles at the extremes of the measurement range are shown in the inset to Fig. 4. The values of the global

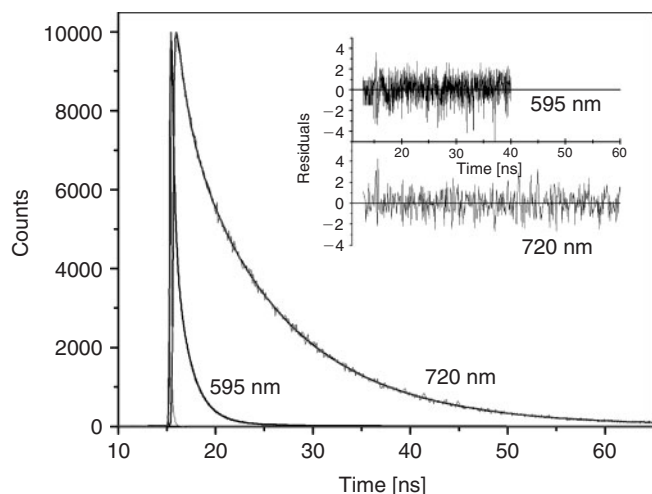


Fig. 4. Fluorescence decay profiles of **1** in toluene with detection wavelengths of 595 and 720 nm. Fitting functions (solid lines) to the profiles and an instrument response function (IRF – dashed line) are also shown. The inset shows the residuals of the fits to the decay profiles resulting from a global fitting of nine decay profiles recorded over the emission spectrum. The fitting function comprised three exponential decay components convolved with the IRF (see text).

fluorescence decay times for two of the decay components are 1.6 and 10.2 ns, indicating that fluorescence attributable to each of the porphyrin species (ZnP and FbP, respectively) is present.

The fractional contributions of the three decay components to the initial amplitude of each decay profile (i.e. the pre-exponential factors) over the detection wavelength range are given in Fig. 5. The components with decay times of 1.63 and 10.2 ns show wavelength-dependence characteristics consistent with the steady-state emission spectra of ZnP and FbP, respectively, with the 10.2-ns component contributing more significantly at longer wavelengths. The third component shows a similar dependence on detection wavelength to the 1.63-ns component but has a much shorter decay time constant of 270 ps, suggesting that it, too, originates from the ZnP chromophores but is quenched. The data in Fig. 5 are also replotted in the Accessory Publication (Fig. A2a) in terms of the relative total intensity of light emitted by each decay time component as a function of detection wavelength. Confirmation that the decay components arise from the two different porphyrins present is obtained by normalizing these values to the total steady-state emission of the pentamer over the emission wavelength range. These are plotted in Figs A2b and c and clearly show spectral characteristics consistent with an assignment of FbP for the 10.2-ns component and ZnP for the 1.63-ns and 270-ps components.

The observation from the star-burst pentamer **1** of a quenched fluorescence lifetime component originating from ZnP in the time-resolved fluorescence decay profiles provides additional evidence that an efficient non-radiative EET process is occurring from some of the peripheral ZnPs to the central FbP. EET from ZnP to FbP is an energetically favourable process (the S1 state of FbP is estimated to lie 0.15 eV lower in energy than ZnP based on steady-state absorption and emission spectra). The decay lifetime of 270 ps corresponds to a rate constant of $3.7 \times 10^9 \text{ s}^{-1}$ for EET and an 83% quenching efficiency of the ZnP fluorescence. The efficiency (E) for the transfer of energy from a photoexcited donor chromophore to an acceptor chromophore via an induced dipole–dipole interaction is dependent on

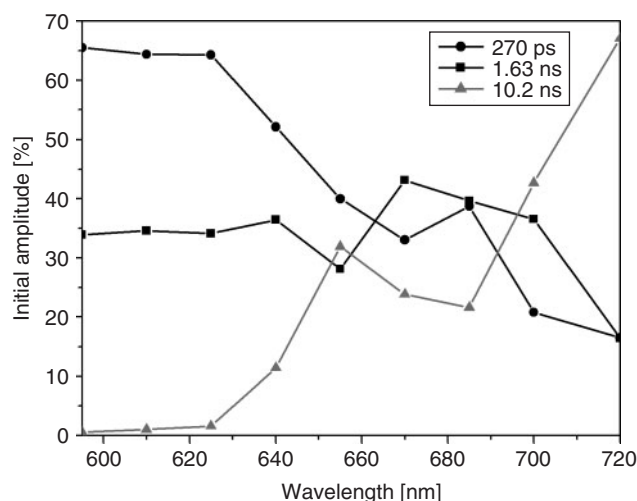


Fig. 5. Pre-exponential factors (i.e. contributions to initial intensity) of the three exponential decay components as a function of detection wavelength for **1** in toluene. The pre-exponential factors were obtained from global fitting of nine decay profiles over the range of 595–720 nm.

the inverse sixth power of the distance (R) between the donor and acceptor chromophores,

$$E = \frac{R_0^6}{R_0^6 + R^6}, \quad (1)$$

where R_0 (the Förster critical transfer distance) is the distance at which 50% of the excitation energy is transferred. R_0 is dependent on the spectral overlap (J) of donor emission and acceptor absorption (with units of $\text{nm}^4 \text{ M}^{-1} \text{ cm}^{-1}$), the donor fluorescence quantum yield (Φ_D), the index of refraction of the medium (η), and a geometrical factor (κ^2) that accounts for the relative orientation of the two interacting transition dipoles. R_0 is given (in Å) by:^[14]

$$R_0 = [8.79 \times 10^{-5} J(\lambda) \Phi_D \eta^{-4} \kappa^2]^{1/6}. \quad (2)$$

Using spectra recorded in toluene for ZnTPP and FbTPP and assuming a random orientation ($\kappa^2 = 0.67$) for the transition dipoles of the ZnP and FbP, Eqn 2 predicts a critical distance of 22.5 Å for energy transfer from ZnTPP to FbTPP. From Eqn 1, it can be calculated that 83% efficiency occurs at a separation of 17.1 Å for this value of R_0 . The values of the pre-exponential factors for the two decay components of ZnP at 615 nm (where there is negligible FbP emission) imply that 40% of all ZnP chromophores are not undergoing EET. Interestingly, the ratio of 3:2 for quenched:unquenched ZnP emission from the pentamer is quite similar to the *cis*:*trans* isomeric ratio of 5:4 determined by NMR studies. This raises the possibility that one geometric isomer, the *cis*-isomer, is undergoing EET while EET in the *trans*-isomer is inefficient. Molecular modelling based on a simple molecular mechanics approach gives the minimum energy centre-to-centre separation for ZnP to FbP in the *cis*-isomer to be 17 Å and for the *trans*-isomer to be 22 Å. This difference, although significant, is not sufficient on its own to effectively ‘switch off’ EET in the *trans*-isomer. As calculated above, 83% efficiency for EET can be expected at 17.1 Å, consistent with the experimental result on the ‘active’ isomer; however, at 22 Å, EET should still be 53% efficient for the other isomer.

The other important factor that will affect the relative EET efficiencies for the two isomers is the relative orientation of the interacting transition dipoles of the ZnP and FbP chromophores. The calculations above are based on a random orientation for which $\kappa^2 = 0.67$. However, κ^2 can take values from 0 to 4 and, clearly, the efficiency of EET is particularly adversely affected as κ^2 tends to zero. κ^2 is given by:^[14]

$$\kappa^2 = [\mathbf{D} \cdot \mathbf{A} - 3(\mathbf{D} \cdot \mathbf{R})(\mathbf{A} \cdot \mathbf{R})]^2, \quad (3)$$

where \mathbf{D} , \mathbf{A} and \mathbf{R} are unit vectors in the directions of the transition dipoles for the donor, the acceptor, and the line connecting the centres of the donor and the acceptor, respectively. It is apparent that κ^2 tends to zero for orthogonal arrangements of \mathbf{D} and \mathbf{A} and, should one of the isomers adopt a conformation where this is the case, it would exhibit very little EET. A factor mitigating this possibility is the flexibility of the linker, which would be expected to lead to significant conformational freedom for each isomer. Another potential complication is the possibility of energy-hopping between the four ZnP chromophores of each pentamer. This would allow an excitation on a poorly oriented ZnP to hop to one where EET is favoured. One way to determine if the observed complexity in photophysical behaviour arises from the presence of geometric isomers and, if so, which isomer is EET active and which is not, would be to study samples with differing *cis:trans* ratios, or ideally, isomerically pure samples. These intriguing possibilities are currently being investigated and will be reported subsequently.

Conclusion

We have been able to demonstrate that selective olefin CM can be effectively applied to the coupling of porphyrin tectons, producing multiporphyrin assemblies in high yield with regio-selective control of metallation sites. The work conducted has also shown that olefin CM can be employed to couple dissimilar porphyrins, both chemo- and stereoselectively, as demonstrated by the formation of a mixed porphyrin pentamer. Steady-state and time-resolved fluorescence studies on the pentamer have shown that significant excitation energy transfer occurs between the peripheral zinc(II) porphyrins and the central free-base porphyrin with a rate constant of $3.7 \times 10^9 \text{ s}^{-1}$. The results also raise the possibility that control of the EET process can be imposed by geometric isomer configurations in the porphyrin array.

Experimental

All chemicals were used as supplied from Aldrich. Solvents were obtained as AR grade reagents and were used as received with the following exceptions. Tetrahydrofuran was stored over Na wire and benzophenone and was distilled before use. Dichloromethane used in reaction was predried over 4-Å sieves, then distilled from CaH. Low resolution-electrospray ionization mass spectrometry (LR-ESIMS) were recorded on a Micromass Platform II API QMS-quadrupole electrospray mass spectrometer. High resolution-ESIMS (HR-ESIMS) were recorded on a Bruker BioApex 47e Fourier-transform mass spectrometer. Laser desorption ionisation mass spectrometry (LDI-MS) were recorded on an Applied Biosystems Voyager-DE STR Biospectrometry workstation. ^1H and ^{13}C NMR spectra were recorded using a Bruker DPX 300 MHz spectrometer (300 MHz, ^1H ; 75 MHz, ^{13}C) or a Bruker DRX 400 MHz spectrometer (400 MHz, ^1H ; 100 MHz, ^{13}C) as solutions in CDCl_3 . Chemical shifts (δ) were calibrated against the residual solvent peak.

Photophysical Measurements

Samples for photophysical measurements were prepared using spectroscopic grade toluene used as received from Aldrich and degassed by multiple freeze–pump–thaw cycles. Steady-state absorption spectra were recorded on a Cary 50 (Varian) spectrophotometer, whereas emission and excitation spectra were obtained on a Cary Eclipse (Varian) fluorimeter. Fluorescence emission decay profiles were recorded using the time-correlated single-photon counting method with excitation provided by the frequency-doubled output (425 nm) of a mode-locked amplified Ti:sapphire laser (Coherent Mira). The system was cavity-dumped to provide a pulse repetition rate of 500 KHz and fluorescence was detected by a multichannel plate photomultiplier (Eldy) and recorded by a photon counting card (Edinburgh Instruments). The time-resolved fluorescence instrumentation has been described extensively elsewhere.^[7b]

Preparation of 5,10,15,20-Tetra(4-(3-butenyl)phenyl)-21H,23H-porphine **2**

A solution of 4-(3-butenyl)benzaldehyde (500 mg, 3.121 mmol) and pyrrole (210 mg, 3.121 mmol) was stirred in propionic acid (15 mL) and refluxed for 3 h. The solution was allowed to cool and the purple precipitate collected, washed with methanol until fresh washings were clear and dried in a cool oven (60°C) to give the *title compound 2* (130 mg, 20%) as a microcrystalline purple solid. δ_{H} (300 MHz, CDCl_3) –2.74 (bs, 2H, inner NH), 2.69 (apparent q, 8H, CH_2), 3.07 (t, J 7.1, 8H, CH_2), 5.19 (m, 8H, alkene H), 6.08 (m, 4H, alkene H), 7.57 (ABq, J 7.7, 8H, ArH), 8.12 (ABq, J 7.7, 8H, ArH), 8.84 (s, 8H, β -pyrrolic H). δ_{C} (75 MHz, CDCl_3) 35.6, 35.9, 112.2, 115.4, 120.3, 127.0, 134.8, 138.4, 140.0, 141.5, 147.8. m/z (HR-ESIMS, +ve, dichloromethane (DCM)/MeOH) Calc. 831.4427. Found 831.4427 [M + H]⁺.

Preparation of 5,10,15,20-Tetrakis(4-(3-butenyl)phenyl)porphyrinato Zinc(II) **4**

To a solution of **2** (54.3 mg, 0.06 mmol) in chloroform (5 mL), saturated zinc acetate in methanol (5 mL) was added and stirred at reflux for 3 h in darkness. On completion, the reaction mixture was quenched with water (25 mL) and transferred to separating funnel. The organics were extracted with chloroform (3 \times 20 mL), washed with water, dried (MgSO_4), filtered, and solvent removed under vacuum to give **4** (54.3 mg, 93%) as a microcrystalline purple solid. Mp >350°C. δ_{H} (300 MHz, CDCl_3) 2.69 (apparent q, 8H, CH_2), 3.07 (t, J 7.1, 8H, CH_2), 5.18 (m, 8H, alkene H), 6.07 (m, 4H, alkene H), 7.56 (ABq, J 7.7, 8H, ArH), 8.12 (ABq, J 7.7, 8H, ArH), 8.95 (s, 8H, β -pyrrolic H). δ_{C} (75 MHz, CDCl_3) 35.6, 35.9, 115.4, 126.8, 132.1, 134.7, 138.5, 140.6, 141.3, 150.5. m/z (HR-ESIMS, +ve, DCM/MeOH) Calc. 915.3376. Found 915.3377 [M + Na]⁺.

Preparation of 5-(4-Hydroxy)phenyl-10,15,20-tris(4-tolyl)-21H,23H-porphine **8**

A solution of (4-hydroxy)benzaldehyde (0.68 g, 5.57 mmol), *p*-tolualdehyde (2.00 g, 16.65 mmol), and pyrrole (1.50 g, 22.30 mmol) was refluxed in propionic acid (150 mL) for 3 h. The solution was allowed to cool overnight and the H_2TTP by-product was removed by suction filtration. Propionic acid was removed from the filtrate by rotary evaporation to leave a black solid. The solid was taken up in ethyl acetate, passed through a short silica plug (SiO_2 , ethyl acetate), and solvent removed under vacuum. Further purification of the crude mixture was

performed by flash chromatography (SiO₂, CHCl₃) to elute any residual H₂TTP; then the solvent system polarity was increased (CHCl₃/MeOH, 20:1), eluting the desired product **8** (320 mg, 8.5%) as a purple solid after solvent removal. Mp >350°C. δ_H (400 MHz, CDCl₃) –2.74 (bs, 2H, inner NH), 2.71 (s, 9H, CH₃), 7.17 (ABq, *J* 8.5, 2H, ArH), 7.55 (ABq, *J* 7.8, 6H, ArH), 8.06 (ABq, *J* 8.5, 2H, ArH), 8.10 (ABq, *J* 7.8, 6H, ArH), 8.86 (s, 8H, β-pyrrolic H). δ_C (100 MHz, CDCl₃) 21.7, 113.9, 119.8, 120.3, 127.6, 134.7, 135.1, 135.9, 137.5, 139.6, 155.6. *m/z* (HR-ESIMS, +ve, DCM/MeOH) Calc. 673.2967. Found 673.2957 [M + H]⁺.

Preparation of 5-(4-Acryloyloxy)phenyl-10,15,20-tris(4-tolyl)-21H,23H-porphine 5

The porphyrin **8** (150.0 mg, 0.297 mmol) and triethylamine (0.1 mL, 0.74 mmol) were combined in freshly distilled THF (50 mL) under an Ar environment. The solution was cooled to 0°C and a THF solution of acryloyl chloride (0.20 mL in 10 mL) was added dropwise over a 15-min period. The reaction mixture was stirred at room temperature for 24 h and then quenched with water (20 mL). The THF was removed by rotary evaporation and the reaction mixture was transferred to a separating funnel. The product was extracted with chloroform (3 × 50 mL), washed with saturated NaHCO₃ (3 × 50 mL), then water (1 × 50 mL), dried (MgSO₄), filtered, and solvent removed by rotary evaporation. Further purification was performed by column chromatography (SiO₂, hexane/CHCl₃, 1:1), giving the desired product **5** (180 mg, 84%) as a pink-purple solid. Mp >350°C. δ_H (400 MHz, CDCl₃) –2.74 (bs, 2H, inner NH), 2.71 (s, 9H, CH₃), 6.15 (dd, *J* 10.4, 1.1, 1H, alkene H), 6.52 (dd, *J* 17.3, 10.4, 1H, alkene H), 6.79 (dd, *J* 17.3, 1.1, 1H, alkene H), 7.56 (m, 8H, ArH), 8.11 (ABq, *J* 7.9, 6H, ArH), 8.25 (ABq, *J* 8.5, 2H, ArH), 8.88 (m, 8H, β-pyrrolic H). δ_C (100 MHz, CDCl₃) 118.8, 120.0, 120.5, 127.7, 128.4, 133.0, 134.7, 135.5, 137.6, 139.5, 140.2, 150.7, 164.9. *m/z* (HR-ESIMS, +ve, DCM/MeOH) Calc. 727.3068. Found 727.3061 [M + Na]⁺.

Preparation of 5-(4-Acryloyloxy)phenyl-10,15,20-tris(4-tolyl)porphinato Zinc(II) 6

The porphyrin **5** (75 mg, 103.1 μmol) was dissolved in chloroform (10 mL) and combined with saturated Zn(OAc)₂ in acetonitrile (5 mL) under an Ar atmosphere. The reaction mixture was stirred at room temperature 24 h in darkness. After this time, the solvent was removed by rotary evaporation and redissolved in chloroform, washed with water (3 × 50 mL), dried (MgSO₄), filtered, and solvent volume reduced. Further purification was performed by column chromatography (SiO₂, CHCl₃) to give the desired product **6** (57 mg, 70%) as a pink-purple solid. Mp >350°C. δ_H (400 MHz, CDCl₃) 2.71 (s, 9H, Ar CH₃), 6.15 (dd, *J* 10.4, 1.2, 1H, alkene H), 6.24 (dd, *J* 17.3, 10.4, 1H, alkene H), 6.53 (dd, *J* 17.3, 1.2, 1H, alkene H), 7.55 (m, 8H, ArH), 8.11 (ABq, *J* 7.9, 6H, ArH), 8.24 (ABq, *J* 8.6, 2H, ArH), 8.97 (m, 8H, β-pyrrolic H). δ_C (100 MHz, CDCl₃) 21.6, 119.6, 119.7, 121.3, 121.4, 127.4, 128.2, 131.8, 132.0, 132.2, 132.8, 134.4, 135.2, 137.2, 139.9, 140.6, 150.1, 150.4, 150.5, 164.7. *m/z* (HR-ESIMS, +ve) Calc. 788.2124. Found 788.2123 [M]⁺.

Preparation of Tetra Methylacrylate-Functionalized Zinc(II) Butenyl Porphyrin 7

The porphyrin **4** (10 mg, 11.2 μmol), and second-generation Grubbs' catalyst (1.9 mg, 2.2 μmol) were combined under an

Ar environment. Degassed CH₂Cl₂ (15 mL) and methyl acrylate (20 mg, 0.225 mmol) were added via syringe and the mixture was left to stir at room temperature for 3 days in darkness. After this time, the solvent was removed by rotary evaporation and the crude material was run through a short plug of silica (CHCl₃/acetone, 20:1). The porphyrinic material was further purified by preparative TLC (SiO₂, CHCl₃), giving the title compound as a red-purple solid **7** (8 mg, 63%). Mp >350°C. δ_H (300 MHz, CDCl₃) 2.86 (apparent q, 8H, CH₂), 3.14 (t, *J* 7.5, 8H, CH₂), 3.80 (s, 12H, CO₂CH₃), 6.02 (dt, *J* 15.8, 1.5, 4H, alkene H), 7.23 (dt, *J* 15.8, 6.8, 4H, alkene H), 7.29 (ABq, *J* 8.7, 8H, ArH), 8.13 (ABq, *J* 8.7, 8H, ArH), 8.86 (m, 8H, β-pyrrolic H). δ_C (100 MHz, CDCl₃) 34.3, 34.6, 51.7, 121.1, 122.0, 126.7, 132.1, 134.8, 140.2, 141.0, 148.6, 150.5, 167.3. *m/z* (LR-ESIMS, +ve) Calc. 1125.4. Found 1125.5 [M + H]⁺.

Preparation of the Mixed Tetra Zinc(II) Porphyrin Pentamer 1

The porphyrins **6** (21.5 mg, 27.2 μmol) and **2** (3.8 mg, 4.5 μmol) were combined with second-generation Grubbs' catalyst (7.7 mg, 9.1 μmol) in CH₂Cl₂ (10 mL, degassed) under an Ar atmosphere and left to stir at room temperature in darkness. The reaction was monitored by TLC, with a new spot appearing at lower R_f value. After 24 h, the solvent was removed by rotary evaporation and column chromatography was performed. Excess **6** was collected first (SiO₂, CHCl₃), then the solvent system changed (CHCl₃/acetone, 50:1) and the desired pentamer **1** eluted as the second band as a pink-red solid (14.7 mg, 84%) after rotary evaporation. Mp >350°C. δ_H (400 MHz, CDCl₃) –2.66 (bs, 2H, inner NH), 2.69 (bs, 36H, CH₃), 2.80 (apparent q, 4H, CH₂), 2.90 (apparent q, 4H, CH₂), 3.09 (t, *J* 7.6, 4H, CH₂), 3.19 (t, *J* 7.6, 4H, CH₂), 6.08 (d, *J* 15.7, 2H, alkene H), 6.24 (m, 2H, alkene H), 7.40–7.63 (m, 36H, ArH and alkene H (hidden)), 8.10 (m, 24H, ArH), 8.22 (m, 8H, ArH), 8.97 (m, 40H, β-pyrrolic H). δ_C (100 MHz, CDCl₃) 21.7, 34.4, 119.8, 119.9, 121.6, 127.0, 127.5, 132.0, 132.2, 132.4, 134.6, 135.0, 135.4, 140.5, 150.4, 150.7, 150.8, 165.0. *m/z* (LDI-MS, no matrix) Calc. 3880.16. Found 3880.05.

Accessory Publication

Figures showing relative fraction of light emitted by each fluorescence decay component for **1** as a function of detection wavelength, the weighted by total steady state emission of **1** at each wavelength in toluene are available from the Journal's website.

Acknowledgements

The present research was supported by the Australia Research Council's Discovery Grant Scheme (DP0878220). CPW thanks the Monash University Faculty of Science for support through a Dean's post-graduate scholarship. TDMB thanks the University of Melbourne for the award of the Faculty of Science Centenary Fellowship. Assistance from Sheryll Yap in carrying out the photophysical measurements is also acknowledged.

References

- [1] (a) S. Prathapan, T. E. Johnson, J. S. Lindsay, *J. Am. Chem. Soc.* **1993**, *115*, 7519. doi:10.1021/JA00069A068
(b) D. Kim, A. Osuka, *Acc. Chem. Res.* **2004**, *37*, 735. doi:10.1021/AR030242E
(c) Y. Nakamura, N. Aratani, A. Osuka, *Chem. Soc. Rev.* **2007**, *36*, 831. doi:10.1039/B618854K

- (d) H. Imahori, *J. Phys. Chem. B* **2004**, *108*, 6130. doi:10.1021/JP038036B
- (e) A. Lyubimtsev, Z. Iqbal, M. Hanack, *Aust. J. Chem.* **2008**, *61*, 273. doi:10.1071/CH07449
- (f) A. C. Benniston, A. Harriman, *Mater. Today* **2008**, *11*, 26. doi:10.1016/S1369-7021(08)70250-5
- [2] (a) K. S. Kim, J. M. Lim, A. Osuka, D. Kim, *J. Photochem. Photobiol. Chem.* **2008**, *1*, 13.
- (b) K. Ogawa, Y. Kobuke, *J. Photochem. Photobiol. Chem.* **2006**, *7*, 1. doi:10.1016/J.PHOTOCHEMREV.2006.03.001
- (c) S. Easwaramoorthi, S. J. Y. Jang, Z. S. Yoon, J. M. Lim, C.-W. Lee, C.-L. Mai, Y.-C. Liu, C.-Y. Yeh, J. Vura-Weis, M. R. Wasielewski, D. Kim, *J. Phys. Chem. A* **2008**, *112*, 6563. doi:10.1021/JP801626S
- [3] (a) C. G. Oliveri, S. T. Nguyen, C. A. Mirkin, *Inorg. Chem.* **2008**, *47*, 2755. doi:10.1021/IC702150Y
- (b) M. L. Merlau, M. P. Meija, S.-T. Nguyen, J. T. Hupp, *Angew. Chem. Int. Ed.* **2001**, *40*, 4239. doi:10.1002/1521-3773(20011119)40:22<4239::AID-ANIE4239>3.0.CO;2-E
- (c) Z. Clyde-Watson, A. Vidal-Ferran, L. J. Twyman, C. J. Walter, D. W. J. McCallien, S. Fanni, N. Bampos, R. S. Wylie, J. K. M. Sanders, *N. J. Chem.* **1998**, *22*, 493. doi:10.1039/A709199K
- (d) V. F. Slagt, P. W. N. M. van Leeuwen, J. N. H. Reek, *Angew. Chem. Int. Ed.* **2003**, *42*, 5619. doi:10.1002/ANIE.200352525
- [4] (a) R. Paolesse, F. Mandoj, A. Marini, C. Di Natale, in *Encyclopedia of Nanoscience and Nanotechnology* (Ed. H. S. Nalwa) **2004**, Vol. 9, p. 21 (American Scientific: Valencia, CA).
- (b) G. D. Fallon, S. J. Langford, M. A.-P. Lee, E. Lygris, *Inorg. Chem. Commun.* **2002**, *5*, 715. doi:10.1016/S1387-7003(02)00550-6
- (c) M. U. Winters, E. Dahlstedt, H. E. Blades, C. J. Wilson, M. J. Frampton, H. L. Anderson, *J. Am. Chem. Soc.* **2007**, *129*, 4291. doi:10.1021/JA067447D
- (d) L. Flamigni, V. Heitz, J.-P. Sauvage, *Struct. Bond.* **2006**, *121*, 217. doi:10.1007/430_018
- (e) M. Fujitsuka, D. Won Cho, N. Solladié, V. Troiani, H. Qiu, T. Majima, *J. Photochem. Photobiol. A* **2007**, *188*, 346. doi:10.1016/J.PHOTOCHEM.2006.12.034
- (f) C. G. Oliveri, S. T. Nguyen, C. A. Mirkin, *Inorg. Chem.* **2008**, *47*, 2755. doi:10.1021/IC702150Y
- [5] (a) P. Thamyongkit, A. Z. Muresan, J. R. Diers, D. Holten, D. F. Bocian, J. S. Lindsey, *J. Org. Chem.* **2007**, *72*, 5207. doi:10.1021/JO070593X
- (b) M. Hoffmann, C. J. Wilson, B. Odell, H. L. Anderson, *Angew. Chem. Int. Ed.* **2007**, *46*, 3122. doi:10.1002/ANIE.200604601
- (c) W. J. Youngblood, T. A. Moore, A. L. Moore, D. Gust, T. E. Mallouk, *J. Am. Chem. Soc.* **2009**, *131*, 926. doi:10.1021/JA809108Y
- (d) A. Satake, J. Tanihara, Y. Kobuke, *Inorg. Chem.* **2007**, *46*, 9700. doi:10.1021/IC7010056
- (e) R. F. Kelley, S. J. Lee, T. M. Wilson, Y. Nakamura, D. M. Tiede, A. Osuka, J. T. Hupp, M. R. Wasielewski, *J. Am. Chem. Soc.* **2008**, *130*, 4277. doi:10.1021/JA075494F
- (f) H. Kai, S. Nara, K. Kinbara, T. Aida, *J. Am. Chem. Soc.* **2008**, *130*, 6725. doi:10.1021/JA801646B
- [6] For a comprehensive overview of porphyrin covalent linkage methods, see the following reviews and references therein. (a) A. K. Burrell, D. L. Officer, P. G. Pileger, D. C. W. Reid, *Chem. Rev.* **2001**, *101*, 2751. doi:10.1021/CR0000426
- (b) M. O. Senge, J. Richter, *J. Porphyr. Phthalocyanines* **2004**, *8*, 934.
- (c) S. Horn, K. Dahms, M. O. Senge, *J. Porphyr. Phthalocyanines* **2008**, *12*, 1053.
- [7] (a) S. J. Langford, M. J. Latter, C. P. Woodward, *Org. Lett.* **2006**, *8*, 2595. doi:10.1021/OL060867N
- (b) T. D. M. Bell, K. P. Ghiggino, A. Haynes, S. J. Langford, C. P. Woodward, *J. Porphyr. Phthalocyanines* **2007**, *11*, 455.
- [8] A. K. Chatterjee, T.-L. Choi, D. P. Sanders, R. H. Grubbs, *J. Am. Chem. Soc.* **2003**, *125*, 11360. doi:10.1021/JA0214882
- [9] (a) P. C. M. van Gervan, J. A. A. W. Elemans, J. W. Gerritsen, S. Speller, R. J. M. Nolte, A. E. Rowan, *Chem. Commun.* **2005**, 3537
- (b) J. M. Bakker, S. J. Langford, M. J. Latter, K. A. Lee, C. P. Woodward, *Aust. J. Chem.* **2005**, *58*, 757. doi:10.1071/CH05262
- (c) C. Ikeda, A. Satake, Y. Kobuke, *Org. Lett.* **2003**, *42*, 1121.
- (d) A. Satake, M. Yamamura, M. Oda, Y. Kobuke, *J. Am. Chem. Soc.* **2008**, *130*, 6314. doi:10.1021/JA801129A
- (e) K.-T. Youm, S. T. Nguyen, J. T. Hupp, *Chem. Commun.* **2008**, 3375. doi:10.1039/B800063H
- [10] It has been reported that the allyl ether functionality is prone to isomerization under metathesis conditions; see R. G. E. Coumans, J. A. A. W. Elemans, P. Thordason, R. J. M. Nolte, A. E. Rowan, *Angew. Chem. Int. Ed. Engl.* **2003**, *42*, 650. doi:10.1002/ANIE.200390179
- [11] J. W. Buchler, in *The Porphyrins* (Ed. D. Dolphin) **1978**, Vol. 1A, p. 389 (Academic: New York, NY).
- [12] (a) P. G. Seybold, M. Gouterman, *J. Mol. Spectrosc.* **1969**, *31*, 1. doi:10.1016/0022-2852(69)90335-X
- (b) D. J. Quimby, F. R. Longo, *J. Am. Chem. Soc.* **1975**, *97*, 5111. doi:10.1021/JA00851A015
- (c) F. R. Hopf, D. G. Whitten, in *Porphyrins and Metalloporphyrins* (Ed. K. M. Smith) **1975**, p. 667 (Elsevier: Amsterdam).
- (d) M. Gouterman, in *The Porphyrins* (Ed. D. Dolphin) **1978**, Vol. 3, p. 1 (Academic: New York, NY).
- [13] (a) L. Pekkarinen, H. Linschitz, *J. Am. Chem. Soc.* **1960**, *82*, 2407. doi:10.1021/JA01495A001
- (b) A. T. Gradyushko, M. P. Tsvirko, *Opt. Spectrosc. (USSR)* **1971**, *31*, 291.
- (c) O. Ohno, Y. Kaizu, H. Kobayashi, *J. Chem. Phys.* **1985**, *82*, 1779. doi:10.1063/1.448410
- [14] (a) T. Förster, *Naturwiss.* **1946**, *33*, 166. doi:10.1007/BF00585226
- (b) T. Förster, *Ann. Phys.* **1948**, *437*, 55. doi:10.1002/ANPD.19484370105